HHS Public Access

Author manuscript

J Thorac Cardiovasc Surg. Author manuscript; available in PMC 2018 July 01.

Published in final edited form as:

J Thorac Cardiovasc Surg. 2017 July ; 154(1): 32–43.e1. doi:10.1016/j.jtcvs.2017.03.053.

Aortic sinus flow stasis likely in valve-in-valve transcatheter aortic valve implantation

Hoda Hatoum, BS[1], **Brandon Moore, PhD**[2], **Pablo Maureira, MD, PhD**[3], **Jennifer Dollery, RN**[4], **Juan Crestanello, MD**[4], and **Lakshmi Prasad Dasi, PhD**[1,2,4]

[1]Department of Biomedical Engineering, The Ohio State University, Columbus, OH, USA

[2]Department of Mechanical Engineering, Colorado State University, Fort Collins, CO, USA

[3]Department of Cardiovascular Surgery CHU de Nancy, Nancy, France

[4]Department of Surgery, The Ohio State University, Columbus, OH, USA

Abstract

Objective—Valve in valve (ViV) procedures using transcatheter aortic valves (TAV) are increasingly performed to treat degenerated bioprosthetic surgical aortic valves (SAV) due to being less invasive than redo aortic valve replacement. The objective of this study is to quantify the changes in aortic sinus blood flow dynamics before and after ViV to gain insight into mechanisms for clinical and sub-clinical thrombosis of leaflets.

Methods—A detailed description of the sinus hemodynamics for ViV implantation was performed in-vitro. A Medtronic Hancock II porcine bioprosthesis was modeled as SAV and a Medtronic CoreValve and Edwards Sapien were used as the TAVs. High-resolution particle image velocimetry (PIV) was employed to compare the flow patterns from these two valves within both the left coronary and non-coronary sinuses in vitro.

Results—Velocity and vorticity within the surgical valve sinuses reached peak values of 0.7 m/s and 1000 s^{-1}, with a 70% decrease in peak fluid shear stress near the aortic side of the leaflet in the non-coronary sinus. With the introduction of TAV, peak velocity and vorticity were reduced to around 0.4 m/s and 550 s^{-1} and 0.58 m/s and 653 s^{-1} without coronary flow and 0.60 m/s and 631 s^{-1} and 0.81 m/s and 669 s^{-1} with coronary flow for CoreValve and Sapien ViV respectively. Also, peak shear stress was around 38% higher along the aortic side of the coronary vs non-coronary TAV leaflet.

Conclusions—Decreased flow and shear stress in ViV indicates higher risk of leaflet thrombosis secondary to flow stasis in the non-coronary sinus.

Address for correspondence and reprints: Lakshmi Prasad Dasi, Ph D, Associate Professor, Department of Biomedical Engineering, The Ohio State University, 473 W 12th Ave., Columbus, OH 43210, TEL: (614) 247-8313, lakshmi.dasi@osumc.edu.

Conflict of Interest: Conflicts of interest were reported in the disclosure forms submitted.

Keywords

aortic sinus; transcatheter aortic valve implantation; calcification; thrombosis

Introduction

Elderly patients with a degenerated surgical bioprosthetic aortic valve are being increasingly considered for a valve in valve (ViV) procedure using a transcatheter aortic valve (TAV) due to its less invasive nature compared to conventional re-do aortic valve replacement surgery(1). However, recent studies have shown a common occurrence of thrombosis related leaflet immobilization in TAV (2–4). In our recent letter, we eluded to one physical mechanism supported by meta-analysis of data focused on observed thrombosis on leaflets(5). It is therefore critical to further investigate the detailed hemodynamics of the ViV configuration to elucidate the underlying hemodynamic mechanism and predict risk of thrombosis in future ViV procedures.

TAVs constitute a relatively new and exciting technology in the field of valvular heart disease. Though it is currently only approved for patients with a high risk of surgical complications, such as the elderly and those with severe comorbidities, it is widely being adopted for ViV use as a viable alternative for re-do aortic valve surgery in patients with a failing bioprosthetic valve. The challenges that the ViV paradigm faces stem from some complications associated mainly with the underlying principles of TAV technology itself. Chief among these complications is the difficulty of placement. This difficulty can lead to breaking off of tissue as well as numerous other detrimental effects(6) like blockage of coronary arteries(7,8), paravalvular regurgitation as well as unfavorable hemodynamic environments that leave the patient susceptible to stroke (9,10).

In this study we seek to provide a detailed and quantitative description of the sinus hemodynamics in the case of ViV implantation and characterize the effects of left coronary flow on the possibility of sinus flow stasis. Sinus flow governs leaflet washout and its characteristics in a ViV configuration can pose additional likelihood of stasis compared to conventional TAV implantation due to the additional narrowing of the aortic annulus from the sewing ring and the presence of stent-posts that interact with the sinus blood flow. Evaluating the mechanistic effects of this arrangement, particularly from the standpoint of sinus hemodynamics may give an insight into the significant risk of leaflet thrombosis and its subsequent role in elevating gradients. (11–13).

Methods

Full details of our methodology are published elsewhere (14,15) in the context of another study. Briefly, 2D particle image velocimetry (PIV) experiments were conducted to visualize aortic sinus flow corresponding to an isolated bioprosthetic heart valve (BPV) configuration and subsequently two ViV arrangements in vitro. Velocity fields were captured within the non-coronary and coronary sinuses. The hemodynamic performance of these configurations was assessed in a pulse duplicator setup under physiological pressure (120/80 mmHg) and flow (5 L/min)[11]. A total number of 10 cycles was performed for each valve setup.

Valve Models

A 23 mm Medtronic Hancock II T505 (Medtronic, Minneapolis, MN, USA) porcine bioprosthetic aortic valve was mounted inside a clear, acrylic sinus chamber machined to mimic the outer walls of the aorta (see Supplementary Figure 1), based on Yap et al (16). The Hancock valve was used as a model for an isolated bioprosthetic implanted aortic valve and tests were run with and without a transcatheter aortic valve (TAV) inserted into this isolated valve configuration.

The TAVs used were a 26mm Medtronic CoreValve and a 23mm Edwards Sapien, which were chosen to match annular size with the isolated bioprosthetic valve. Their positions relative to the isolated bioprosthetic valve were determined based on clinical findings, which suggest an ideal TAV leaflet location that extends just downstream of the BPV valve leaflets (17). The CoreValve was chosen to be placed sub-annularly with respect to the BPV annulus. This valve combination and TAV placement location also compare well with published recommendations for valve-in-valve implantation (18,19).

Results

Differences in flow patterns between the isolated bioprosthetic valve coronary and non-coronary sinuses have already been analyzed and discussed in detail in our previous work (15).

Coronary Flow Profile

Coronary flow waveforms are presented in Supplementary Figure 2 for the isolated bioprosthetic configuration as well as the ViV configurations. As shown in the figure, coronary flow is slightly reduced during systole in the presence of the TAV. The diastolic portions of the flow waveforms were not significantly different.

Qualitative Sinus Flow Visualization

High resolution PIV was employed to measure and analyze the hemodynamics for six sinus cases: (1) isolated BPV configuration non-coronary, (2) isolated BPV configuration coronary, (3) CoreValve ViV configuration non-coronary, (4) CoreValve ViV configuration coronary, (5) Sapien ViV configuration non-coronary and (6) Sapien ViV configuration coronary. Qualitative “streak” images were created for each case by computing a sliding average and subtracting the sliding minimum over ten frames at a time. Depictions of camera and laser orientation as well as viewing the orientation of the results are shown in Supplementary Figure 3. Corresponding videos of these particle streaks are included for one complete cardiac cycle for isolated BPV non-coronary, isolated BPV coronary, CoreValve ViV non-coronary, CoreValve ViV coronary, Sapien ViV non-coronary and Sapien ViV coronary configurations. Still-frame snapshots from these videos are included in Figure 1.

The results for the isolated bioprosthetic valve configuration control cases are shown for the non-coronary (Figure 1a) and coronary (Figure 1d) sinuses. During early systole, forward flow in each of these cases is significant and sinus flow velocity is high. A stagnation point near the downstream end of the sinus wall where flow is split either diverted towards the

sinotubular junction or recirculated back into the sinus appears. This point is located slightly farther upstream in the coronary sinus and migrates downstream in both cases as systole progresses. At mid systole, a flow from the back of the sinus takes place and then gets drawn into the coronary artery which is absent in the non-coronary sinus case. Near the end of systole, the sinus vortex has grown, however the flow velocity is significantly reduced. During diastole, sinus flow velocities are much lower. There is a pattern of flow toward the base of the sinus at early diastole, but by mid diastole the flow is relatively stagnant. In the coronary sinus, early and mid-diastole display particle motion that is mainly toward the ostium, with this pattern being stronger and more widespread throughout the sinus toward mid diastole.

Having a ViV setup greatly alters sinus hemodynamics (Figures 1b and 1c). There is little to no streamwise flow within the sinus during early systole, however a small vortex is shed off the leaflet tip in the CoreValve ViV compared with a flow following the sinus wall contour and starting at the sinotubular junction in the Sapien ViV. This vortex grows in size and starts to fill more of the sinus as systole progresses. In the Sapien ViV, the flow starts to fill the sinus until the leaflet edge. However, the flow speed is much lower for both ViV configurations for these portions of systole. Diastolic hemodynamics are similar with and without ViV.

Coronary flow in the ViV cases causes some changes in sinus hemodynamics from the non-coronary ViV case (Figures 1e and 1f). During early stages of systole in the CoreValve ViV, the sinus vortex covers much more of the sinus. In the Sapien ViV, the flow tracks the sinus contour more obviously. However, flow does not recirculate completely but rather exits the sinus at the coronary ostium leading to no noticeable sinus vortex toward the end of systole. Similarly, both early and mid-diastolic hemodynamics show a dominant pattern of flow from all parts of the sinus towards the coronary ostium, with somewhat higher velocities during mid diastole.

Quantitative Flow Results

The velocity vectors and vorticity contours are presented at select time-points of interest in Figures 2 and 3. In the BPV configuration (Figure 2a and 3a), the presence of the sinus vortex is clear in the early stages of systole. The center of this vorticity is just downstream of the leaflet tip, in between the edge of the leaflet and the sinus wall. The velocity of the significant forward flow that enters the sinus reaches around 1.3 m/s and the peak vorticity magnitude around 800 s^{-1}. Most of this is diverted into the aorta by the curvature of the downstream sinus wall while a small portion is redirected back toward the base of the sinus. At mid systole, the sinus vortex is still clearly distinguished but has migrated slightly downstream. Vorticity magnitude is greatest at this time point, with a peak around 1000 s^{-1} and vortex velocities on the order of 0.7 m/s. Late systole induces a reduction in the overall sinus velocity and therefore vorticity magnitude. However a weakened sinus vortex is still present, which is the dominant sinus flow pattern as most streamwise flow no longer exists within the sinus In the coronary sinus, the major velocity and vorticity magnitudes during diastole exist only near the ostium.

The most dramatic difference caused by the introduction of a TAV to the BPV (Figures 2b and 2c) is a reduction in overall velocity and vorticity magnitudes, which becomes noticeable during early systole. Also, the less noticeable sinus vortex is positioned more downstream in the TAV cases than in the BPV case. At mid systole, the sinus vortex size is relatively unchanged as it stretches from the sinotubular junction to the tip of the TAV leaflet. Vorticity magnitude also remains similar to that during early systole, with a peak around 550 s^{-1} in the CoreValve ViV and 653 s^{-1} in the Sapien ViV. Velocity magnitude is reduced relative to the BPV case, with highest systolic values around 0.4 m/s and 0.58 m/s in the CoreValve and Sapien ViV respectively.

Velocity and vorticity were also calculated for the coronary sinus for the ViV configurations (Figures 3b and 3c). In this case, the sinus vortex plays much less of a role in the CoreValve ViV. For instance, at early systole the highest velocity and vorticity magnitude occur due to flow entering the coronary ostium, with velocity magnitude in this region around 0.3 m/s. In the Sapien ViV, the flow is directed by the coronary flow so the motion at the sinus wall is more defined compared to the non-coronary case. At early systole, the highest velocity magnitude is around 0.45 m/s. Around mid-systole, hemodynamics are not significantly changed, however there is stronger recirculation around the downstream sinus wall and some capturing of the flow into the ostium is apparent. Once forward velocity has slowed, towards the end of systole, there is only a weak recirculating flow pattern present and a relatively small amount of coronary perfusion. Coronary flow is still low during early diastole but increases by mid diastole, reaching velocities near 0.4 m/s and 0.53 m/s in the CoreValve and Sapien ViV respectively.

Shear Stress Distribution

Shear stress was calculated at the given time points of interest for each valve case. Results are presented as contour maps in Figures 4 and 5 that give an indication on the order of magnitude of shear stresses in the sinus. The sub-region near the leaflet is of particular interest since low leaflet wall shear stress may be linked to flow stasis.

BPV configuration sinus shear stress patterns are displayed in Figure 4a and 5a. During early systole, most of the sinus is dominated by large magnitude negative (acting downward relative to respect to leaflet surface) shear stress, over 1 Pa magnitude, in the downstream end of the sinus. However, there is also a significant region of strong positive shear adjacent to the leaflet free edge, which extends to the aortic side of the leaflet in the coronary cases. During diastole, significant shear stress only exists near the edges of the ostium in the coronary sinus.

In the ViV configurations, sinus shear stress levels are generally reduced compared to the BPV cases (Figures 4b and 4c). During systole, in the CoreValve ViV two distinct shear regions are noticeable: one negative region along the aortic side of the TAV leaflet and another positive region along the sinus wall. Stress magnitude in these regions increases during mid systole and then decreases dramatically during late systole. In the Sapien ViV, the two distinct shear regions along the aortic side of the TAV and along the sinus wall are clear in early systole. Similar to the CoreValve ViV, stress magnitudes in these shear regions increase during mid-systole and decrease during late systole. However, the pattern becomes

more intersected at peak systole and dissipates in late systole with a more dominating negative region. There is very little shear stress in the sinus throughout diastole for the ViV non-coronary cases.

Shear stresses for the ViV coronary sinus case are presented in Figures 5b and 5c. In the CoreValve ViV, there is higher magnitude shear stress near the leaflet tip and the ostium than in the non-coronary sinus (Figure 5b). The same observation applies to the Sapien ViV near the ostium and inside the sinus compared with the non-coronary case (Figure 5c) only this maximum shear stress region does not occur near the leaflet of the TAV. This observation is more noticeable in the coronary case compared to the non-coronary one.

Figure 6a and 6b show the probability density function of flow shear stress magnitude in the sub-region adjacent to the leaflets (see inset) during systole and diastole respectively. As is clearly evident from this figure, higher shear stresses (> 1.5 Pa) occur in the BPV cases during systole alone. For the CoreValve ViV cases, coronary flow appears to slightly augment the likelihood of even higher shear stresses (>1.5 Pa). For the ViV cases shear stresses do not exceed about 1.4 Pa during systole. During diastole, the shear stress is < 1.6 Pa, with the non-coronary cases yielding a higher probability of shear stress exceeding 0.5 Pa but less than 1.6 Pa. For the Sapien ViV non-coronary case during systole, higher shear stress magnitudes than 0.5 Pa likelihood drops drastically near the leaflet region. However, shear stress reaches magnitudes up to 1.8 Pa compared to 1.1 Pa for the non-coronary CoreValve ViV. Coronary flow seems to have a significant impact on the shear stress probability distribution. High shear stress values have a high likelihood of occurrence near the leaflets before a gradual drop occurs. During diastole, the probability of having high magnitudes of shear stress decreases with the coronary flow yielding a higher probability of occurrence of higher magnitudes of shear stress near the leaflets. In systole and diastole, the Sapien ViV shows a drastic drop in the likelihood of having shear stress ranging from 0.5 to 1.0 Pa and 0.2 to 0.5 Pa in systole and diastole respectively compared to patterns shown for the CoreValve ViV and the BPV in the non-coronary cases.

Table 1 encompasses leaflet washout velocity and mean shear stress magnitude in the region neighboring the leaflets in each valve case and shows the impact of coronary and non-coronary flow presence in addition to the differences between BPV and ViV. Also, mean values of pressure gradients that are in accordance with literature (19) are reported to be 5.01±0.0064, 17.05±0.14 and 17.67±0.27 mmHg for the BPV, CoreValve ViV and Sapien ViV respectively. Because ViV setups especially with BPVs with sewing rings compromise the annulus area, add more structures that alter the basic fluid dynamics (attachment and separation points and shear layers) the pressure gradients are expected to be higher. The pressure gradient difference between the Sapien and the CoreValve ViV is not significant however, the BPV pressure gradient is drastically different as the leaflets are in good condition.

Discussion

Here we focus our discussion mainly on how ViV changes aortic sinus hemodynamics and its potential relevance to prosthetic leaflet washout and leaflet opening in the context of

understanding the mechanisms for leaflet thrombosis, in addition to highlighting the differences in sinus hemodynamics between CoreValve and Sapien ViV.

ViV Hemodynamic Effects

Examination of detailed sinus flow patterns for the ViV cases yields numerous differences from the isolated bioprosthetic valve configuration. Both ViV vortices are much weaker overall than the isolated bioprosthetic valve configuration vortex with that of the Sapien ViV being stronger than that of the CoreValve ViV but concentrated more downstream away from the leaflets.

The differing vorticity dynamics between these two valve cases are regulated largely by geometric and structural changes. When no TAV is present, the leaflet tip opens into the sinus during early systole. In the presence of a CoreValve, on the other hand, the leaflet extends farther downstream and is restricted from opening completely by the stent frame. The extended length of the TAV leaflet is likely the reason for the downstream location at which the vortex develops, while the constant vortex topology is due to the static BPV leaflet location. With the presence of the Sapien in ViV, the leaflets do not extend far much beyond those of the BPV and the vortex develops downstream away from the leaflets which highlights the more significant impact of the stent structure.

The vortex structure is also due to viscous effects as well as geometry. These effects and their impact on vortex formation and development are explained for general sinus flow by Yap et al (16). In summary, a vortex forms within a sinus by: 1) some of the freestream flow entering the sinus or 2) shear force interaction between sinus fluid and the freestream flow. In the present study, it appears that 1) is responsible for the BPV case sinus vortex and 2) is responsible for the ViV sinus vortices. This means that no freestream flow enters the sinus in the ViV cases, which could be due to the extension of the leaflet in the case of the CoreValve ViV, the restriction of leaflet opening by the stent, by the stent itself, or by a combination of these factors. Regardless of the cause, the absence of freestream flow in the ViV case sinus leads to a much weaker vortex, with flow shear being the sole contributing factor behind vortex formation. Additionally, some quiescent fluid near the BPV leaflet is entrained by the vortex, thus increasing overall fluid motion from early to mid-systole.

Altered vorticity dynamics due to the implantation of a TAV could have implications for disease. This is mainly due to the low magnitude and downstream location of the TAV sinus vortex. Low magnitude means low blood velocity and therefore low shear stress along the leaflet – a factor that is strongly linked to leaflet thrombosis. Likewise, a downstream vortex that only slightly reaches the base of the sinus leaves a pocket of nearly stagnant fluid for much of the cardiac cycle. This particular finding is in agreement with results from a study by Ducci et al (20). Such stagnation zones are often associated with thrombosis, which could explain an increased risk of leaflet thrombosis and elevated gradients for patients with TAV (9,10).

ViV Hemodynamic Effects in a Coronary Sinus

Most alterations in hemodynamics brought about by TAV implantation within the BPV occur in both non-coronary and coronary sinuses. However, some hemodynamic changes are

unique to the coronary sinus. Flow into the ostium represents a much larger portion of fluid movement in the sinus. Furthermore, this added flow could help alleviate thrombosis risk in the coronary sinus of ViV patients, a mechanism we elude to explain preferential leaflet thrombosis only in leaflets that are protected from the benefits of coronary flow(5).

Shear Stress

Leaflet wall shear stress is often of interest in aortic valve studies due to its correlation to thrombosis as well as calcification in native and prosthetic leaflets. While no wall shear stress was calculated in this study, fluid shear stress within the sinus was calculated and represents the scale of magnitude of wall shear stresses at leaflet at different times during the cardiac cycle.

Coronary presence alone alters some sinus shear stress patterns in the isolated bioprosthetic valve configuration mainly the leaflet. When examining this region in both cases, it is apparent that there is higher magnitude shear for the coronary sinus. Additionally, shear stress direction is constant for the coronary case while it changes direction for the non-coronary case. Both of these trends have implications for disease since reduced and oscillatory shear stresses are correlated to development of thrombosis or calcification (21). Therefore, the non-coronary sinus appears hemodynamically more susceptible thrombosis and/or calcification than the coronary sinus, which is supported by clinical findings that show earlier and more frequent signs of calcification on the non-coronary leaflet (22).

When examining the effects of the ViV arrangement on shear stress in the sinus the most noticeable trend is that much lower magnitude shear stress occurs for the ViV valve cases. Such a large reduction in shear could lead to accelerated calcification of the prosthesis leaflets and growth of thrombosis leading to leaflet mobility problems (2,5).

Coronary presence significantly increases sinus shear stresses in the ViV sinus throughout the cardiac cycle, most notably along the aortic side of the leaflet. This could be caused by a low pressure region near the ostium that helps pull the vortex toward the upstream end of the sinus. Lower ostial pressure (“sink hole effect”) also produces some shear stress in the base of the sinus from entrainment of otherwise stagnant flow at the base into the ostium from this region.

Conclusion

In conclusion, this study constitutes a detailed look at aortic sinus hemodynamics as regulated by a valve-in-valve arrangement, analyzed with and without the presence of a coronary ostium. Novel methodology was developed and validated to simulate coronary flow in vitro. Sinus flow patterns were greatly altered with the introduction for the ViV cases. Peak sinus flow velocity was reduced by 40% and 17% in the CoreValve and Sapien ViV respectively and a particular lack of flow was discovered near the annulus in both ViV cases. These trends could help explain the increased risk of leaflet thrombosis in ViV patients. However, the coronary sinus demonstrated higher flow velocities and wall shear stresses than the non-coronary sinus, meaning this sinus is less susceptible to thrombus formation.

Limitations

This study was performed in vitro in a rigid aortic chamber using one size for each of the TAVs used to fit in the BPV with leaflets within the post, 26mm Medtronic CoreValve and 23mm Edwards Sapien. Future studies will entail surgical BPVs with leaflets on the outside of the post.

Supplementary Material

Refer to Web version on PubMed Central for supplementary material.

Acknowledgments

Funding: This work was partially supported by NIH under Award Number R01HL119824, and the American Heart Association under award 11SDG5170011.

Funding Sources

The authors gratefully acknowledge funding from National Institutes of Health (NIH) under Award Number R01HL119824, and the American Heart Association under award 11SDG5170011. The content is solely the responsibility of the authors and does not necessarily represent the official views of the NIH or AHA.

GLOSSARY OF ABBREVIATIONS

BPV	Bioprosthetic Heart Valve
PIV	Particle Image Velocimetry
SAV	Surgical Aortic Valve
TAV	Transcatheter aortic valve
ViV	Valve in Valve

References

1. Bapat V, Attia R, Redwood S, et al. Use of transcatheter heart valves for a valve-in-valve implantation in patients with degenerated aortic bioprosthesis: technical considerations and results. The Journal of thoracic and cardiovascular surgery. 2012; 144:1372–1380. [PubMed: 23140962]
2. Makkar RR, Fontana G, Jilaihawi H, et al. Possible Subclinical Leaflet Thrombosis in Bioprosthetic Aortic Valves. New England Journal of Medicine. 2015; 373:2015–2024. [PubMed: 26436963]
3. De Marchena E, Mesa J, Pomenti S, et al. Thrombus Formation Following Transcatheter Aortic Valve Replacement. Jacc-Cardiovascular Interventions. 2015; 8:728–739. [PubMed: 25946447]
4. De Marchena E, Mesa J, Pomenti S, et al. Thrombus Formation Following Transcatheter Aortic Valve Replacement (vol 8, pg 728, 2015). Jacc-Cardiovascular Interventions. 2015; 8:1140–1141.
5. Hatoum H, Crestanello J, Dasi LP. Possible Subclinical Leaflet Thrombosis in Bioprosthetic Aortic Valves. New England Journal of Medicine. 2016; 374:1590–1592.
6. Groves EM, Falahatpisheh A, Su JL, Kheradvar A. The Effects of Positioning of Transcatheter Aortic Valves on Fluid Dynamics of the Aortic Root. ASAIO. 2014; 60:545–552.
7. Dvir D, Webb J, Brecker S, et al. Transcatheter Aortic Valve Replacement for Degenerative Bioprosthetic Surgical Valves: Results From the Global Valve-in-Valve Registry. Circulation. 2012; 126:2335–2344. [PubMed: 23052028]

8. Stanger O, Gisler F, Londono MC. Valve-in-valve: Estimating the risk of ostium obstruction in failed sorin stentless valves. The Journal of thoracic and cardiovascular surgery. 2015; 149:644–645. [PubMed: 25726886]
9. Waksman R, Minha Sa. Stroke After Aortic Valve Replacement: The Known and Unknown. Circulation. 2014; 129:2245–2247. [PubMed: 24690610]
10. Smith CR. Transcatheter versus surgical aortic-valve replacement in high-risk patients. The New England journal of medicine. 2011; 364:2187. [PubMed: 21639811]
11. Fanning JP, Wesley AJ, Platts DG, et al. The silent and apparent neurological injury in transcatheter aortic valve implantation study (SANITY): concept, design and rationale. Bmc Cardiovascular Disorders. 2014:14. [PubMed: 24483947]
12. Brown ML, Park SJ, Sundt TM, Schaff HV. Early thrombosis risk in patients with biologic valves in the aortic position. The Journal of thoracic and cardiovascular surgery. 2012; 144:108–111. [PubMed: 21864857]
13. Tseng EE. When valve-in-valve implantation is not sufficient: Bioprosthetic Russian dolls. The Journal of thoracic and cardiovascular surgery. 2016; 152:624–625. [PubMed: 27130303]
14. Moore B, Dasi LP. Spatiotemporal complexity of the aortic sinus vortex. Exp Fluids. 2014:55.
15. Moore BL, Dasi LP. Coronary flow impacts aortic leaflet mechanics and aortic sinus hemodynamics. Annals of biomedical engineering. 2015; 43:2231–2241. [PubMed: 25636598]
16. Yap CH, Saikrishnan N, Tamilselvan G, Yoganathan AP. Experimental measurement of dynamic fluid shear stress on the aortic surface of the aortic valve leaflet. Biomechanics and Modeling in Mechanobiology. 2012; 11:171–182. [PubMed: 21416247]
17. Lichtenstein SV, Cheung A, Ye J, et al. Transapical transcatheter aortic valve implantation in humans - Initial clinical experience. Circulation. 2006; 114:591–596. [PubMed: 16880325]
18. Bapat VN, Attia RQ, Condemi F, et al. Fluoroscopic Guide to an Ideal Implant Position for Sapien XT and CoreValve During a Valve-in-Valve Procedure. Jacc-Cardiovascular Interventions. 2013; 6:1186–1194. [PubMed: 24139931]
19. Azadani AN, Reardon M, Simonato M, et al. Effect of Transcatheter Aortic Valve Size and Position on Valve-in-Valve Hemodynamics: An In-Vitro Study. The Journal of Thoracic and Cardiovascular Surgery.
20. Ducci A, Tzamtzis S, Mullen MJ, Burriesci G. Hemodynamics in the Valsalva Sinuses after Transcatheter Aortic Valve Implantation (TAVI). Journal of Heart Valve Disease. 2013; 22:688–696. [PubMed: 24383382]
21. Chandra S, Rajamannan NM, Sucosky P. Computational assessment of bicuspid aortic valve wall-shear stress: implications for calcific aortic valve disease. Biomechanics and Modeling in Mechanobiology. 2012; 11:1085–1096. [PubMed: 22294208]
22. Freeman RV, Otto CM. Spectrum of calcific aortic valve disease - Pathogenesis, disease progression, and treatment strategies. Circulation. 2005; 111:3316–3326. [PubMed: 15967862]

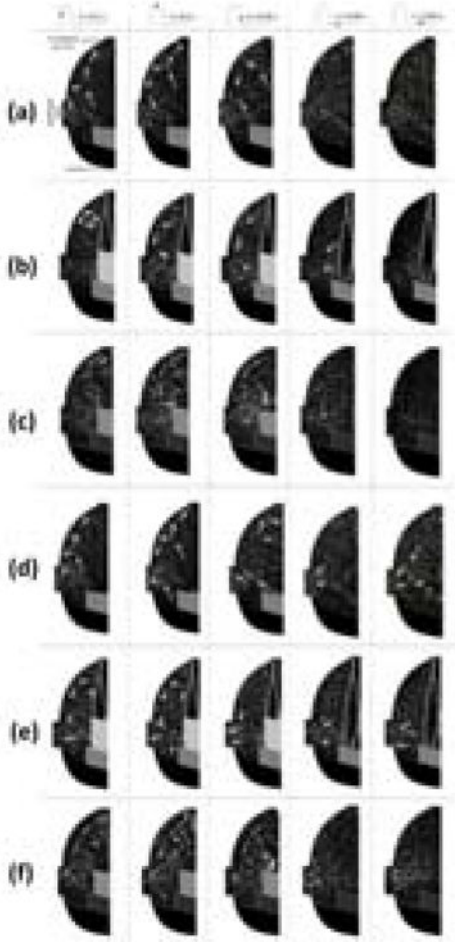

Figure 1.

Snapshots from streak plot videos generated by time bin averaging raw images of non-coronary sinuses for (a) BPV (b) ViV with CoreValve and (c) ViV with Sapien and of coronary sinuses for (d) BPV, (e) ViV with CoreValve and (f) ViV with Sapien. Arrows are manually drawn (not computed vectors) to help depict trends in the videos.

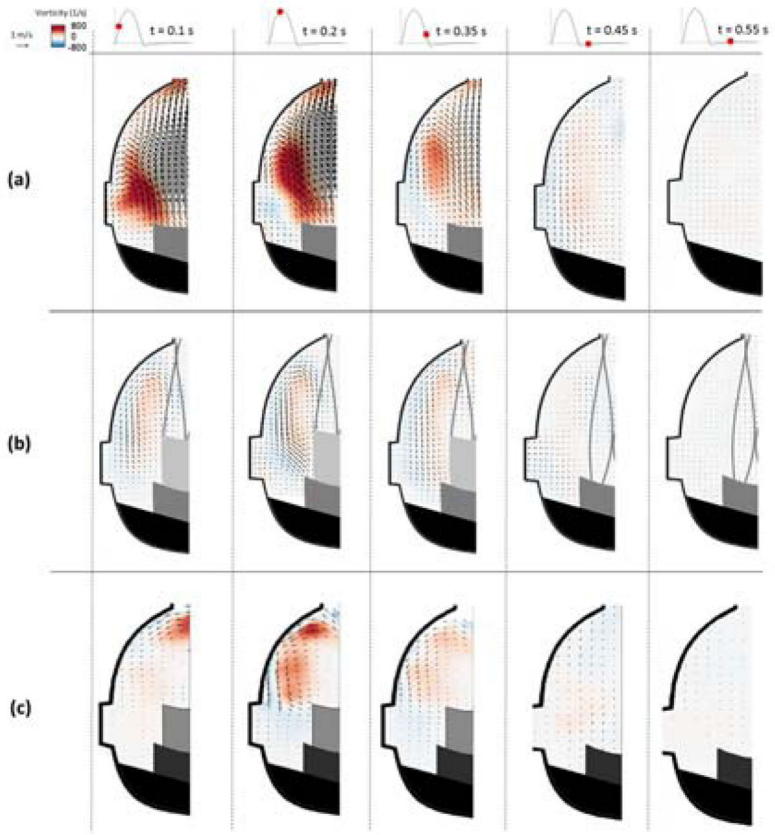

Figure 2.

Velocity vectors and vorticity contours within the non-coronary sinus for (a) BPV (b) ViV with CoreValve and (c) ViV with Sapien for each case at selected time points throughout the cardiac cycle.

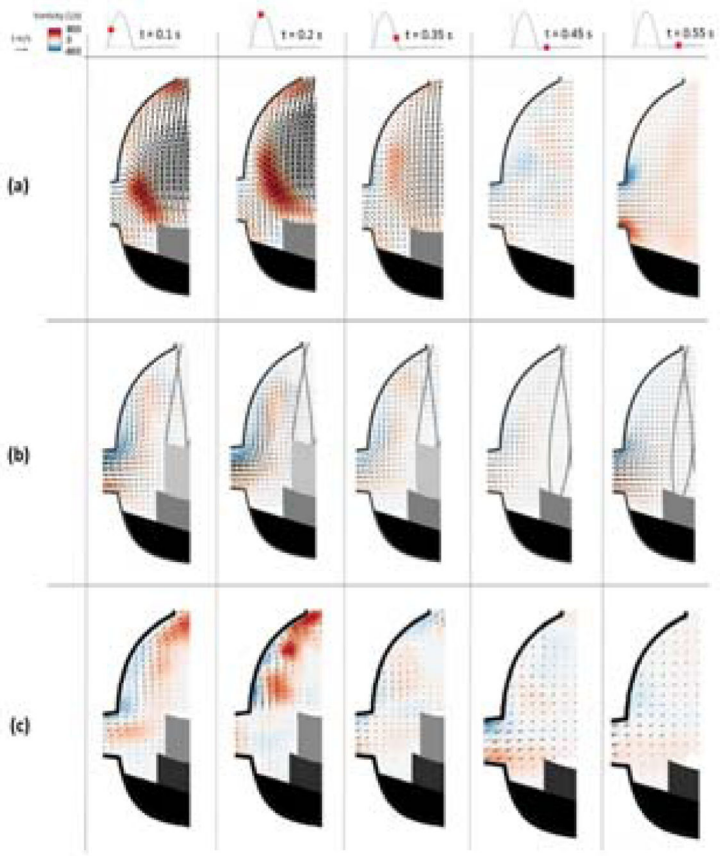

Figure 3.

Velocity vectors and vorticity contours within the coronary sinus for (a) BPV (b) ViV with CoreValve and (c) ViV with Sapien for each case at selected time points throughout the cardiac cycle.

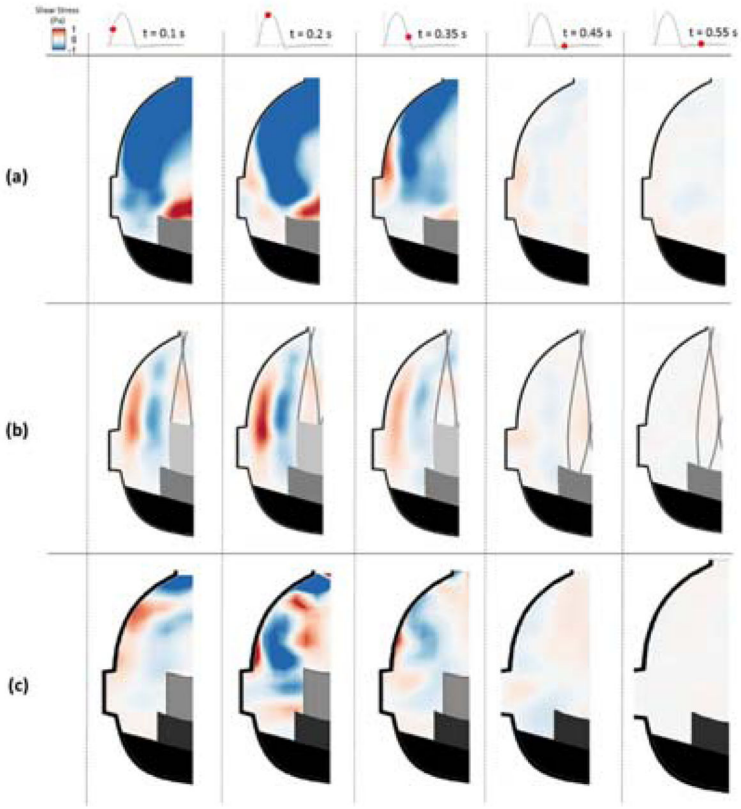

Figure 4.

Shear stress contours within the non-coronary sinus of (a) BPV (b) ViV with CoreValve and (c) ViV with Sapien for each case at selected time points throughout the cardiac cycle.

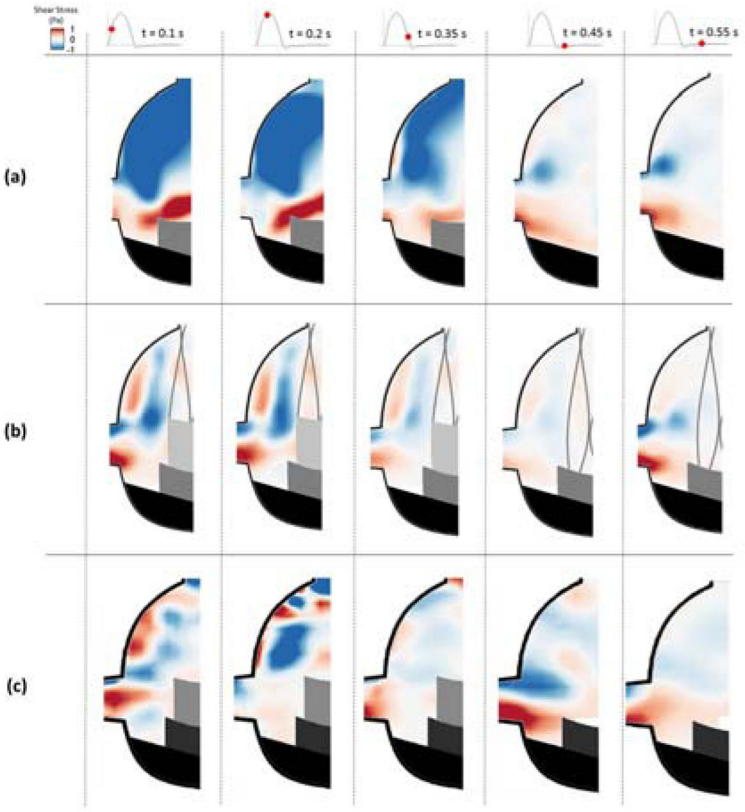

Figure 5.
Shear stress contours within the coronary sinus of (a) BPV (b) ViV with CoreValve and (c) ViV with Sapien for each case at selected time points throughout the cardiac cycle.

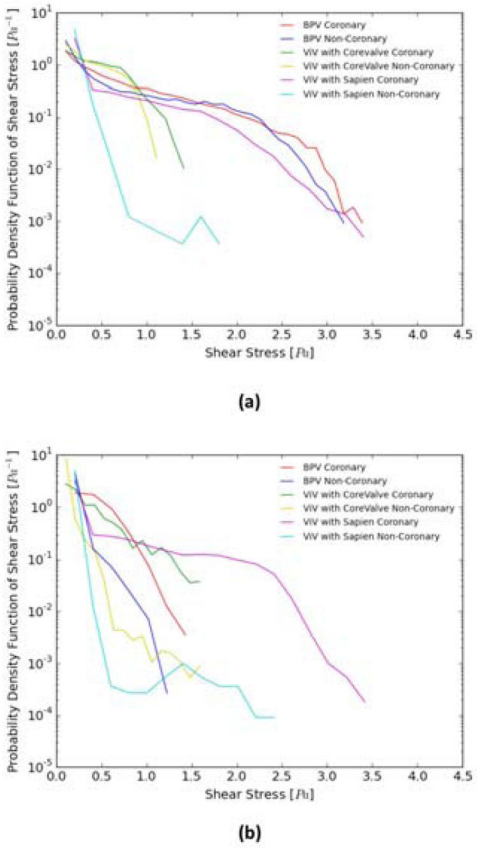

Figure 6.

Probability Density function in log scale of varying shear stress distribution values along a sub-region near the isolated bioprosthetic and ViV configurations leaflets during (a) systole and (b) diastole.

Table 1

Mean shear stress magnitude and mean leaflet washout velocity in the leaflets neighborhood region. Values are mean ± standard deviation.

	Systole - Without Coronary Flow			Diastole - Without Coronary Flow		
	BPV	**CoreValve ViV**	**Sapien ViV**	**BPV**	**CoreValve ViV**	**Sapien ViV**
Leaflet Washout Velocity (m/s)	0.16±0.23	0.12±0.096	0.055±0.072	0.030±0.036	0.023±0.044	0.030±0.034
Mean Shear Stress (Pa)	0.076±0.55	0.014±0.48	0.013±0.067	0.036±0.081	0.023±0.093	0.030±0.052
	Systole – With Coronary Flow			**Diastole - With Coronary Flow**		
	BPV	**CoreValve ViV**	**Sapien ViV**	**BPV**	**CoreValve ViV**	**Sapien ViV**
Leaflet Washout Velocity (m/s)	0.41±0.30	0.19±0.14	0.15±0.10	0.21±0.13	0.20±0.18	0.17±0.090
Mean Shear Stress (Pa)	0.31±0.53	0.12±0.38	0.2±0.63	0.24±0.71	0.078±0.43	0.14±0.28